Biochimica et Biophysica Acta 1840 (2014) 2914–2923

Contents lists available at ScienceDirect

Biochimica et Biophysica Acta

journal homepage: www.elsevier.com/locate/bbagen

# Monitoring the kinetics of CellTrace™ calcein red-orange AM intracellular accumulation with spatial intensity distribution analysis

Zahra Hamrang *[,1], Hayley J. McGlynn [1], David Clarke, Jeffrey Penny, Alain Pluen *

*Manchester Pharmacy School, University of Manchester, Manchester, UK*

ARTICLE INFO

*Article history:*
Received 1 February 2014
Received in revised form 20 May 2014
Accepted 22 May 2014
Available online 29 May 2014

*Keywords:*
Confocal microscopy
Fluorescence correlation spectroscopy
Spatial intensity distribution analysis
Fluorescence

ABSTRACT

*Background:* Routine black box approaches quantify fluorescence intensity to profile the uptake of fluorophores, providing limited insight into microscopic events. Spatial intensity distribution analysis has previously been reported to quantify oligomerisation and number of particles from selected regions and profile intracellular distributions of labelled moieties.
*Methods:* In this study, the concentration and time-dependent behaviour of CellTrace™ calcein red-orange (AM) intracellular accumulation was examined in colorectal adenocarcinoma cell line and bovine aortic endothelial cells. Monolayers were subjected to fluorescence correlation spectroscopy, fluorescence intensity and SpIDA measurements to determine differences in the rate and extent of intracellular accumulation.
*Results:* Intracellular accumulation data derived from Spatial intensity distribution analysis were found to correlate with that of fluorescence correlation spectroscopy and fluorescence intensity profiles. The extent of intracellular accumulation was found to be time and concentration-dependent in both cell lines examined, with no significant differences in the rate of intracellular accumulation.
*Conclusions:* Spatial intensity distribution analysis applied at '*proof of concept*' level is a rapid and user-friendly tool that can be applied to the quantification of intracellular concentration and kinetics of fluorophore uptake.
*General significance:* Confocal imaging as a routinely implemented tool for profiling fluorescently-labelled species is often under-exploited for yielding quantitative parameters.



## 1. Introduction

Epithelial and endothelial *in vitro* models cultivated under physiologically-relevant conditions have proven to be useful in the generation of a wealth of data concerning drug uptake and transcellular distribution to date. Despite the abundance of data generated from such models, the routine application of black-box analytical approaches (e.g. plate readers) limits the direct characterisation of intracellular distributions and any existent heterogeneities occurring within cell monolayers [1].

Over recent decades increasing research has been invested in the development and implementation of microscopic tools (and image analysis algorithms) that can aid elucidation of intracellular phenomena and quantification of ligand uptake. Fluorescence correlation spectroscopy (FCS) was first developed in 1972 by Magde et al. and successfully applied to the diffusion and chemical reaction kinetic measurement of reversible ethidium bromide binding to DNA [2]. Since, FCS has extensively been applied as an established sensitive biophysical method for intracellular single molecule measurements and assessment of aggregation, flow and interactions between molecules [3–5]. However, challenges associated with FCS use relating to sampling volumes (i.e. a confocal volume of femtolitres), the requirement for specialist equipment and focusing of the excitation laser beam within cellular regions (leading to photo-damage) have been deemed factors limiting widespread FCS use in the biophysical characterisation of ligand cellular uptake. Furthermore, the performance of a large number of experiments is required to assure acquisition of sufficient representative (i.e. statistically significant) cell populations [6].

Since the advent of FCS, numerous image analysis tools (e.g. image correlation spectroscopies [7] and photon correlation histogram-based methods [8]) and a diversity of image analysis platforms (e.g. ImageJ [9] and ICY [10]) have been introduced that are compatible with commercial confocal laser scanning microscopes, and provide a means for quantitative spatial and temporal parameterisation of live cell imaging studies. To date confocal microscopy has proven to be a useful tool both in the visualisation and mechanistic assessment of cellular uptake, trafficking and intracellular dynamics of ligands in multiple fields of pharmaceutical and biomolecular research [11–13].

*Abbreviations:* AM, acetoxymethyl; BAEC, bovine aortic endothelial cell; FCS, fluorescence correlation spectroscopy; PMT, photomultiplier tube; ROI, region of interest; SpIDA, spatial intensity distribution analysis

* Corresponding authors.
*E-mail addresses:* Zahra.hamrang@manchester.ac.uk (Z. Hamrang), Alain.pluen@manchester.ac.uk (A. Pluen).

[1] Both authors contributed equally to the manuscript.

http://dx.doi.org/10.1016/j.bbagen.2014.05.014
0304-4165/

For example, spatial intensity distribution analysis (SpIDA) utilised in this study is an image analysis tool reported for the quantification of protein oligomerisation and their relative concentrations (i.e. densities), enabling the determination of concentrations of monomer or oligomeric species within confocal images acquired as time series, single frames or *z*-stack images with a high degree of spatial resolution. Furthermore, in contrast to approaches utilising temporal analysis (e.g. FCS, number and brightness methods and image correlation spectroscopies), SpIDA is not susceptible to effects of photobleaching, autofluorescence and the impact of clustering. Through appropriate sampling strategies it is possible to profile intracellular concentrations of moieties of interest and their sub- and inter-cellular distributions [8,14,15].

With advances in confocal imaging capabilities and the development of image analysis algorithms exploiting fluorescence intensity fluctuations over a large sampling area with sufficient spatial and temporal resolution, quantification of both intracellular dynamics and concentration of fluorophores has become a reality. This is of particular interest in high content screening applications in biological and pharmaceutical research.

Herein, the focus of the current study is to consider the application of SpIDA (in conjunction with FCS and fluorescence intensity measurements) for the assessment of kinetics, extent and heterogeneity of fluorophore uptake and intracellular distribution. Caco-2 cells are routinely utilised to study oral drug absorption due to the expression of brush border enzymes and transporters commonly expressed in the gastrointestinal tract that are of relevance to drug uptake [16–18]. Bovine aortic endothelial cells (BAECs) were also selected in this study to represent a model for studying endothelial cellular uptake.

To demonstrate this concept, uptake and retention of the model compound CellTrace™ calcein red-orange AM and its cleaved product are assessed in Caco-2 cell and BAEC monolayers using a combination of FCS, live cell imaging and subsequent analyses (i.e. fluorescence intensity and SpIDA).

CellTrace™ calcein red-orange AM contains an acetoxymethyl ester (AM) group that masks charge, rendering it non-polar and permeant to live cells. The excitation and emission properties of CellTrace™ calcein red-orange AM do not change appreciably upon loss of the AM groups either by passive or active cleavage through hydrolysis (see Fig. 1). CellTrace™ calcein red-orange is less permeable to leakage compared to the parent molecule (due to charge-based intracellular retention) and is therefore well-retained by live cells that possess intact plasma membranes [19].

## 2. Materials and methods

### 2.1. Materials

Bovine aortic endothelial cells, BAECs (passages 5–10) and Caco-2, colorectal adenocarcinoma cells (passages 50–60), were purchased from Genlantis and ATCC, respectively. All cell culture reagents including Dulbecco's Modified Eagle Medium (DMEM) and CellTrace™ calcein red-orange AM were obtained from Life Technologies (Paisley, UK). Phosphate-buffered saline (PBS) and HEPES (4-(2-hydroxyethyl)-1-piperazineethanesulfonic acid) buffer were acquired from Sigma Aldrich Ltd. (Dorset, UK). Nunc® eight well chamber slides (effective surface area: 0.8 $cm^2$/well) and sodium bicarbonate were obtained from Fisher Scientific (Leicestershire, UK).

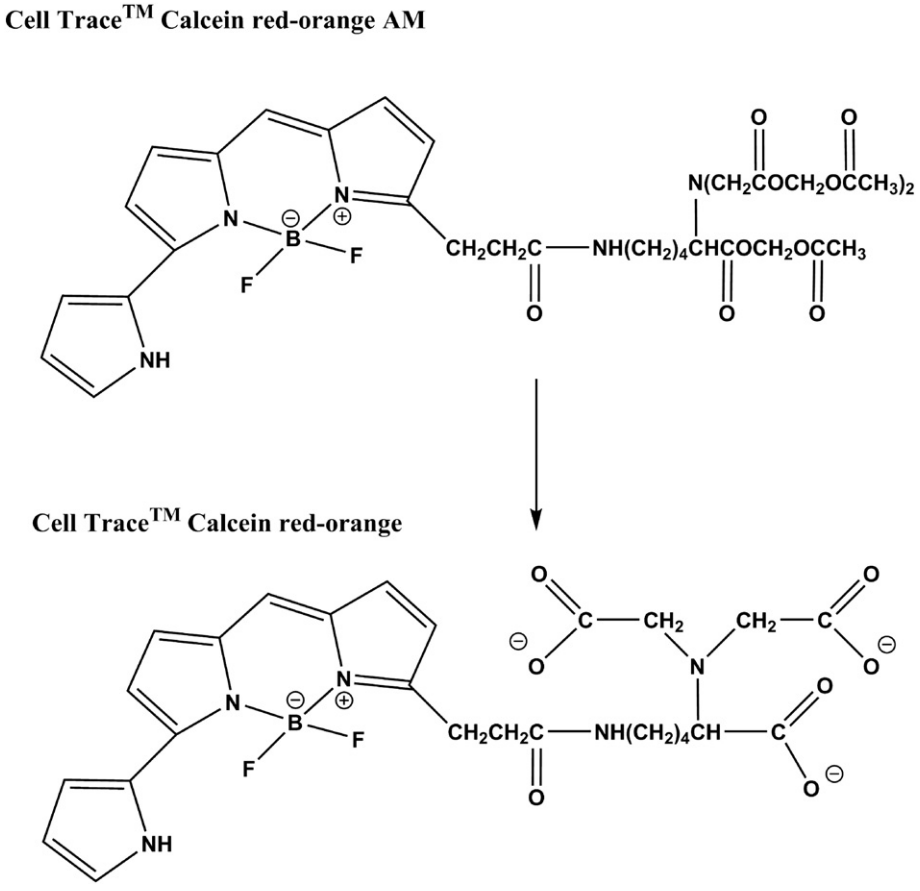


**Fig. 1.** Chemical structure of CellTrace™ calcein red-orange and final cleaved product following cleavage by intracellular esterases.

### 2.2. Methods

#### 2.2.1. Cell culture and sample preparation

Caco-2 cells and BAECs were cultured in DMEM supplemented with 10% (*v*/*v*) heat-inactivated foetal bovine serum (FBS), 1% (*v*/*v*) non-essential amino acids, 4 mM L-glutamine, and 100 IU/ml penicillin/streptomycin, at 37 °C in an atmosphere containing 5% (*v*/*v*) $CO_2$. Cells were detached from the flask when 70% confluent by trypsinisation at 37 °C and the resultant cell suspension centrifuged. The cell pellet was re-suspended in medium and either sub-cultured (1:4) in T-25 flasks or seeded at a density of $10^5$ cells/ml in eight well chamber slides. Cells were incubated at 37 °C in an atmosphere of 5% $CO_2$ for 24 h prior to the performance of uptake/accumulation experiments.

For concentration-dependent experiments, monolayers were rinsed with PBS twice prior to performance of experiments and the growth medium replaced with CellTrace™ calcein red-orange AM diluted in transport medium (i.e. growth medium with 20 mM HEPES buffer and 35.7 mM sodium bicarbonate) to the final concentration (i.e. 10, 25, 50 and 100 nM).

Cell monolayers incubated to the desired time point followed by a triplicate PBS rinse to remove any extracellular CellTrace™ calcein red-orange AM prior to visualisation with confocal microscopy. In the case of time-dependent experiments, the same procedure as above was applied without a rinsing step to monitor temporal changes in intracellular CellTrace™ calcein red-orange (AM) concentration.

#### 2.2.2. FCS cell measurements of intracellular fluorophore accumulation

All FCS measurements were performed using a ConfoCor 2 fluorescence correlation spectrometer (Zeiss, Jena, Germany) with a c-Apochromat 40×/1.2 NA water-immersion objective. Samples were excited with a 543 nm Helium–Neon laser and the resultant fluorescence collected through a 560–615 nm band-pass filter. All FCS cellular measurements (one run of 10 s per cell) were performed following a 10 second pre-bleach (see appendix).

#### 2.2.3. Analysis of FCS data

Intracellular CellTrace™ calcein red-orange (AM) autocorrelation data were fitted to an anomalous diffusion model in OriginPro v8.5.1 software (OriginLab® Corporation, Massachusetts, United States) using Eq. (1) [20,21];

$$G(\tau) = \frac{1/N}{\left[1+\left[\tau/\tau_D\right]^{\alpha}\right]\left[1+1/S^2\left[\tau/\tau_D\right]^{\alpha}\right]^{0.5}} \cdot \left[1+\frac{T}{1-T}e^{-\tau/\tau_T}\right] \quad (1)$$

where $\alpha$ refers to the anomalous exponent, $\tau_T$ the relaxation time of the triplet state and $T$ the fraction of fluorophores residing in the (non-fluorescent) triplet state.

Values were minimised by using a Marquardt algorithm with the structure parameter fixed to 5. Fit quality was assessed on residuals to the fit and correlation coefficient ($R^2$) values, respectively. The number of particles, *N*, was used to assess the intracellular CellTrace™ calcein red-orange (AM) concentration and was determined directly from the amplitude of the autocorrelation curves.

#### 2.2.4. Confocal laser scanning microscopy

Images were acquired using a Zeiss LSM 510 confocal microscope (Jena, Germany) with a c-Apochromat 40×/1.2 NA water-immersion objective lens. CellTrace™ calcein red-orange (AM) was excited using the 543 nm Helium–Neon laser line and fluorescence collected using a 560–615 nm band-pass filter. All confocal images were captured with identical laser power, pinhole diameter, detector and amplifier gain across all experiments. For each experimental condition (e.g. CellTrace™ calcein red-orange AM concentration and period of incubation) several fields of view were captured.

#### 2.2.5. Spatial intensity distribution analysis of confocal images

SpIDA was performed on all live cell images using the method described by Godin et al. [8,15] and the analysis of retention was carried out using the software available for download from the developer website (http://www.neurophotonics.ca/en/tools/software). Images were imported into the SpIDA user interface and the laser beam waist and pixel size inputted followed by photomultiploer tube (PMT) shot noise and white noise values measured as follows:

*Characterisation of photomultiplier tube (PMT) shot noise*. Varying PMT voltage conditions and laser powers may be used to assess the conditions under which direct linearity is existent between the photoelectric current and the measured fluorescence intensity. This is significant since the derived brightness and number of particle parameters following SpIDA analysis of confocal images are influenced by shot noise. This measurement was performed through imaging immobilised pre-bleached beads using a Helium–Neon 543 nm excitation laser and a c-Apochromat 40×/1.2 NA water-immersion objective. The beads were excited over a range of laser powers, at a detector gain of 600 and a pixel dwell time of 3.2 μs (n = 1024 pixels). A slope of 276 IU ($R^2 = 0.941$) was determined from the plot of pixel intensity variance versus mean pixel intensity and applied to all future measurements for images acquired under identical image acquisition conditions.

*Determination of the white noise contribution*. All images were imported into Metamorph® version 7.5 (Molecular Devices, Wokingham, UK) and the image dimensions calibrated. The white noise was measured through selection of extracellular regions of interest (ROIs) and the quantification of corresponding fluorescence intensities prior to image importation into the SpIDA graphical user interface.

*Quantification of number of particles*. The number of CellTrace™ calcein red-orange (AM) particles (per beam waist area) was determined for all ROIs in all confocal images (i.e. *z*-stack and single frame) following corrections for white noise and PMT shot noise.

Super-Poissonian fitting of fluorescence intensity histograms determined from confocal laser scanning microscopy images forms the basis of SpIDA. Quantal brightness and the density per beam area (i.e. number of fluorescent moieties defined within a specified region) are output parameters derived from SpIDA that are achieved through determination of the fluorescence intensity histogram of each pixel fluorescence intensity value within a specified ROI. Histograms are determined from calculating all the possible configurations in which a fluorescent entity may reside in a point spread function (PSF)-defined region. Following weighted calculations of each configuration and its respective probability assuming a Poisson distribution for *N* particles inside the PSF, the fitting function applied to determination of the final histogram is [8,15]:

$$H(\varepsilon, N, k) = \sum_n \rho^n(\varepsilon; k) Poi(n, N) \text{ with } \rho^0(\varepsilon; k) = \delta_{k,0} \quad (2)$$

where *H* is the histogram fitting function that is normalised so that the integral over $\kappa$ equals unity, $\varepsilon$ represents the molecular quantal brightness, *N* the number of particles within the PSF and $\rho^n$ the probability of observing an intensity of light of $\kappa$ (assuming proportionality to the number of emitted photons) by *n* particles of $\varepsilon$ brightness.

*2.2.6. Quantification of the intracellular fluorescence intensity of CellTrace™ calcein red-orange (AM)*

Acquired confocal image *z*-stacks were subsequently deconvolved using the AutoDeblur® software (MediaCybernetics, US). Deconvolved images were subsequently imported into MetaMorph® for analysis of fluorescence intensity. For quantification of the intracellular CellTrace™ calcein red-orange (AM) fluorescence intensity in Caco-2 cells and BAEC monolayers, a minimum threshold intensity was selected for each image (or frame in a *z*-stack in order to exclude contribution of extracellular components to intensity measurements). Integrated fluorescence intensity measurements were subsequently computed for the specified threshold area (and normalised to the thresholded surface area).

*2.2.7. Determination of time-dependent changes in intracellular CellTrace™ calcein red-orange (AM) concentration*

A differential model was applied to intracellular retention where three various states were proposed accounting for uptake, retention (parent and cleaved compound), and the contribution of removal from the cell due to exocytosis (see Fig. 2).

Since the contribution of exocytosis was assumed to be negligible from preliminary FCS measurements over extended time periods (see appendix), a first order process was assumed and an exponential fit (Box Lucas exponential model in OriginPro) applied to the determination of kinetic parameters in time-dependent intracellular measurements.

*2.2.8. Statistical analysis*

Unless stated otherwise, all population samples of intracellular retention were subjected to analysis of variance testing (i.e. $P < 0.05$). Where the number of CellTrace™ calcein red-orange (AM) particles has been stated, this refers to exponentiation of the log mean and in order to determine the upper and lower standard deviations, the log mean ± 1 standard deviation was converted to an exponent. Statistical analyses were performed on data obtained from all methods and experiments as a function of concentration and period of incubation.

*2.2.9. Data analysis*

To facilitate comparison of population data, box plots were utilised in this study. The number of particle data obtained from FCS and SpIDA analyses was inputted into OriginPro (v8.5.1) and box plots were generated (representing the mean, median, upper and lower quartile ranges, range of variables and outliers). Further particulars of box plots and associated calculations (e.g. outliers) can be located on the software developer website (http://www.originlab.com/index.aspx?go=Products/Origin/Graphing/2D&pid=959).

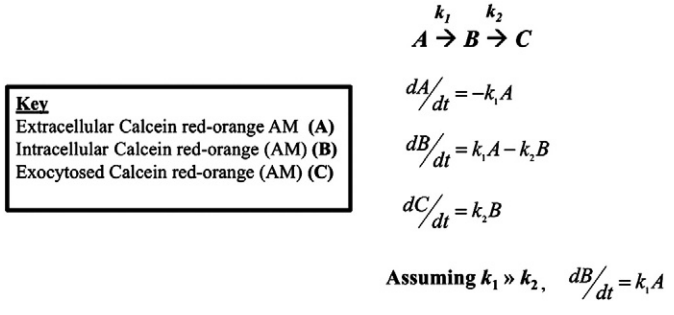


**Fig. 2.** Proposed model for CellTrace™ calcein red-orange (AM) intracellular accumulation: exocytosis contribution to intracellular concentration is assumed to be negligible and only intracellular species of CellTrace™ calcein red-orange (AM) are quantified.

## 3. Results

### 3.1. Optimisation of FCS measurements

*3.1.1. Characterisation of CellTrace™ calcein red-orange AM in solution by FCS*

Fluctuation analysis of CellTrace™ calcein red-orange AM in transport medium revealed a simple monophasic autocorrelation curve. The amplitude of these curves was higher in water and noisier than that of fluorophore dissolved in transport medium (see Fig. 3).

Autocorrelation curves fitted to data from CellTrace™ calcein red-orange AM dissolved in transport medium using a single component model possessed low triplet fractions (i.e. < 12%), resistance to photobleaching following excitation by the laser source and a clean autocorrelation curve shoulder (up to 50 nM CellTrace™ calcein red-orange AM in comparison to water), enabling accurate analysis of number of particles within samples (see appendix).

*3.1.2. Criteria for plane selection in confocal imaging experiments*

To assess variation in intracellular accumulation as a function of cross-section, both SpIDA and fluorescence intensity (a traditional approach) measurements were applied to a single *z*-stack image (Fig. 4).

Data indicates a varied distribution of CellTrace™ calcein red-orange intracellular number of particles as a function of cross-section, with the most variation observed in planes of the highest fluorescence intensity and number of particles. Subsequently, the brightest planes were selected for all two-dimensional imaging experiments of time and concentration-dependent accumulation.

*3.1.3. Time-dependent intracellular accumulation of CellTrace™ calcein red-orange (AM)*

Images obtained from confocal microscopy were analysed using both SpIDA and routine intensity measurements. Fluorescence intensity profiles, SpIDA and FCS demonstrate time-dependent intracellular retention of CellTrace™ calcein red-orange (AM) in both cell lines.

Confocal micrographs of Caco-2 cell and BAEC monolayers incubated with 50 nM CellTrace™ calcein red-orange (AM), exhibited a time-dependent increase in the intracellular concentration of the fluorophore in each cell type (Fig. 5) with a predominant cytoplasmic distribution.

Integrated fluorescence intensity data presented in Fig. 5 indicate a higher extent of CellTrace™ calcein red-orange (AM) retention in Caco-2 cells in comparison to BAECs ($n = 20$) whereas, the reverse trend was observed in the case of SpIDA and FCS output data. The overall trend in intracellular number of particle accumulation with time was consistent between both SpIDA and FCS measurements (Fig. 5C–F). The slopes obtained from an exponential Box Lucas fit (see appendix) of fluorescence intensity data for Caco-2 and BAEC data were 0.16 and 0.24 $min^{-1}$ (with corresponding standard errors of 0.004 and 0.06), respectively. In the case of fits performed on the median number of particles calculated from SpIDA ($R^2 = 0.94$ for Caco-2 and $R^2 = 0.97$ for BAECs), slopes of 0.03 and 0.04 $min^{-1}$ (with a corresponding standard error 0.02 for both cell lines) were determined for Caco-2 cells and BAECs, respectively. Performance of ANOVA ($P < 0.05$) in both cases confirmed that no statistically significant differences in the rate of fluorescence intensity changes were observed between the two cell lines over time.

*3.1.4. Intracellular accumulation of CellTrace™ calcein red-orange (AM) over extended periods*

In order to further assess the ability of SpIDA to determine intracellular concentrations, accumulation following incubation with 50 nM CellTrace™ calcein red-orange AM was assessed for an extended time period (i.e. 60 min) and in a larger population of Caco-2 and BAEC cells (representative confocal images and output parameters from SpIDA and FCS are presented in Fig. 6).

In each confocal image multiple ROIs were selected for analysis and the re-exponentiated mean ± standard deviation expressed as a range.

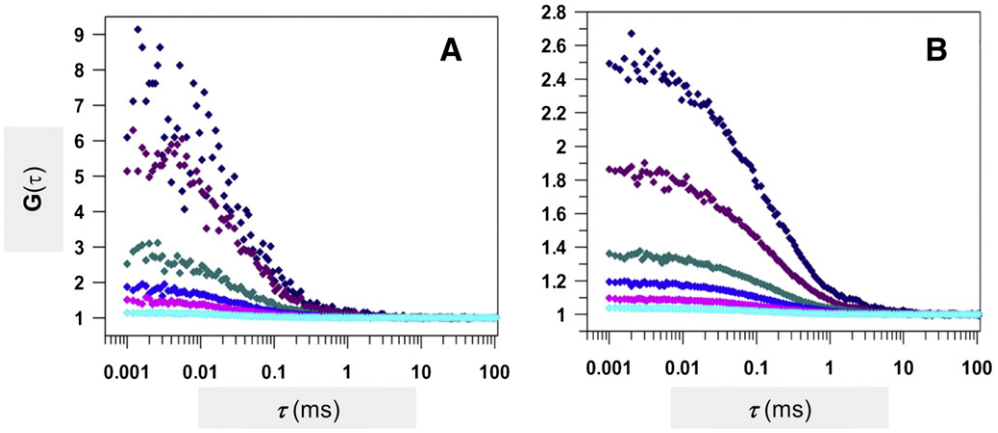


**Fig. 3.** Autocorrelation curves were obtained for 5 (♦), 10 (♦), 25 (♦), 50 (♦), 100 (♦) and 250 nM (♦) CellTrace™ calcein red-orange AM dissolved in water (A) and transport medium (B). All measurements were obtained over 10 successive runs, each consisting of a 10 second acquisition time.

The number of particle (per confocal volume) log-normal distributions is presented for data obtained from SpIDA and separate FCS measurements in both cell lines.

The intracellular numbers of particles per beam area (re-exponentiated mean ± standard deviation of a log-normal distribution) determined from SpIDA following incubation with 50 nM CellTrace™ calcein red-orange AM for 60 min were determined to be $17 < 25 < 38$ and $13 < 21 < 32$ in BAECs and Caco-2 cells, respectively. Hence, data obtained with SpIDA are in good agreement with corresponding ranges obtained from FCS experiments that were $17 < 25 < 37$ and $13 < 20 < 32$ for BAECs and Caco-2 monolayers studied under identical experimental conditions.

SpIDA and FCS data presented in Fig. 6 exhibit a broad distribution in the intracellular accumulation of CellTrace™ calcein red-orange (AM)

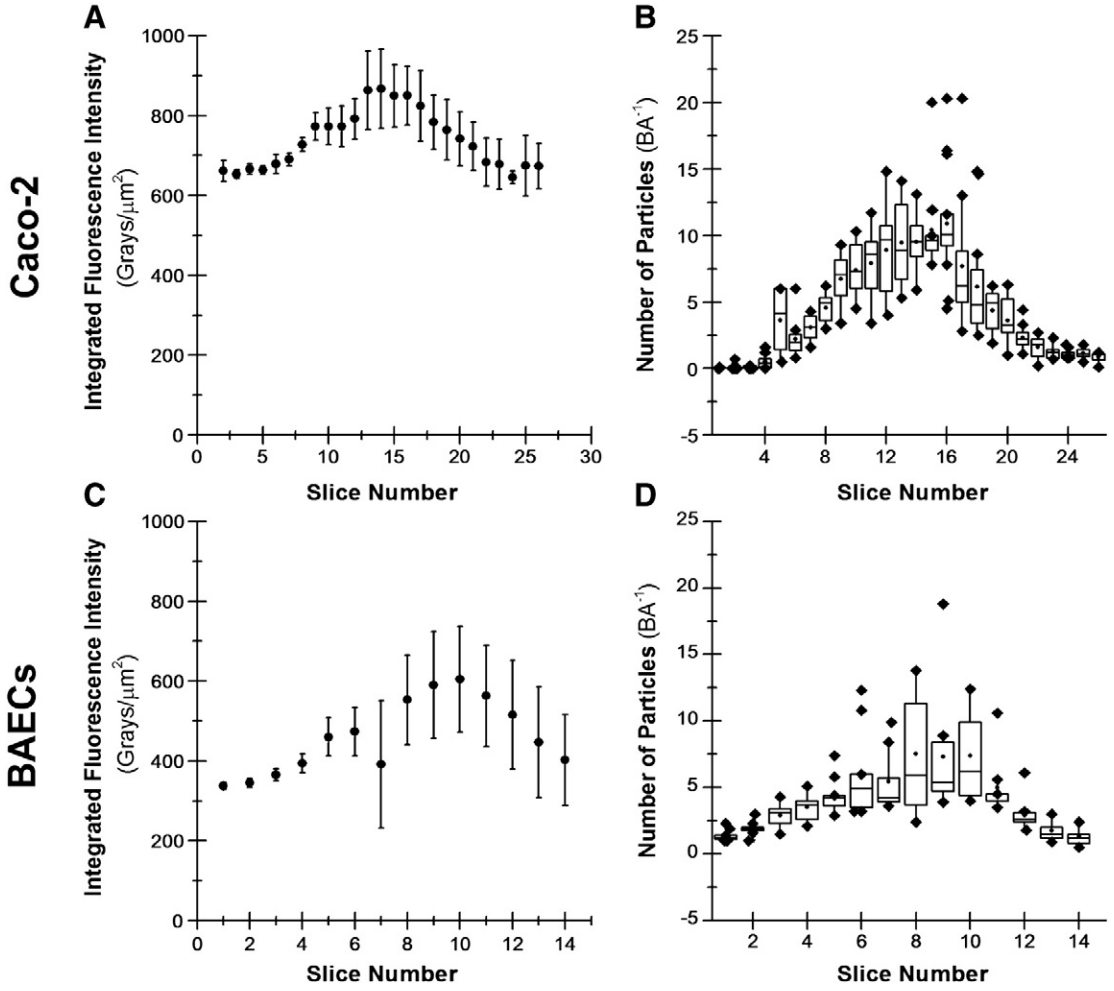


**Fig. 4.** Cross-sectional profile of CellTrace™ calcein red-orange AM (i.e. 50 nM) accumulation in *z*-stack images acquired from Caco-2 and BAEC monolayers incubated up to 60 min. Number of particles per beam area determined using SpIDA for Caco-2 (B) and BAECs (D), and corresponding integrated fluorescence intensities computed with Metamorph® for Caco-2 (A) and BAEC (C) monolayers. The mean is represented by ●, outliers by ♦, and the median, lower and upper quartiles by horizontal lines.

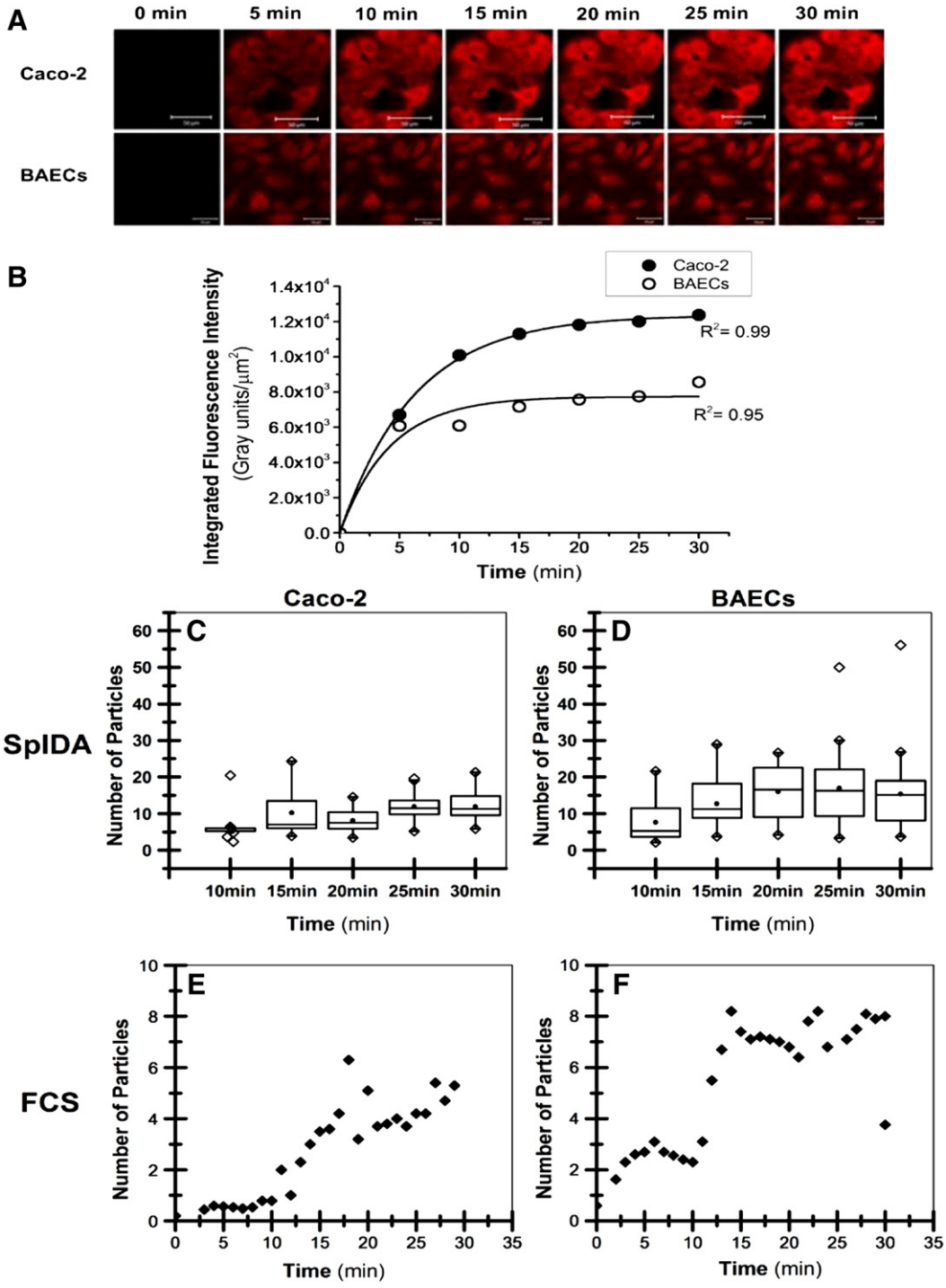


**Fig. 5.** Confocal images representing time-dependent intracellular retention of 50 nM CellTrace™ calcein red-orange (AM) over 30 min (pixel size of 0.44 μm) for Caco-2 cells and BAECs (A), corresponding fluorescence intensity plots (B) SpIDA (C and D) and FCS (E and F) measurements of intracellular CellTrace™ calcein red-orange (AM) number of particles per confocal volume. The mean is represented by (●), the median, upper and lower quartiles are represented by solid horizontal lines and outliers by (◊). Data points obtained from single cell FCS measurements are represented by (♦).

as represented by the box plots. The number of particle data (i.e. FCS and SpIDA) from BAECs and Caco-2 cells suggests cell line-dependent accumulation since a statistically significant ($P < 0.05$) difference was observed between the two sample sets.

### *3.1.5. The effect of concentration on the extent of CellTrace™ calcein red-orange (AM) intracellular accumulation*

In order to assess the influence of CellTrace™ calcein red-orange AM concentration on the extent of intracellular retention, a combination of (confocal) live cell imaging experiments and FCS measurements was performed. Representative images following incubation of Caco-2 and BAEC monolayers with various concentrations of CellTrace™ calcein red-orange AM (i.e. 10, 25, 50 and 100 nM) for a period of 60 min are presented in Fig. 7.

Confocal micrographs showed intracellular distribution of CellTrace™ calcein red-orange (AM) throughout the cells with an observed higher extent of accumulation as the initial concentration of CellTrace™ calcein red-orange AM is increased. Representative confocal images demonstrate

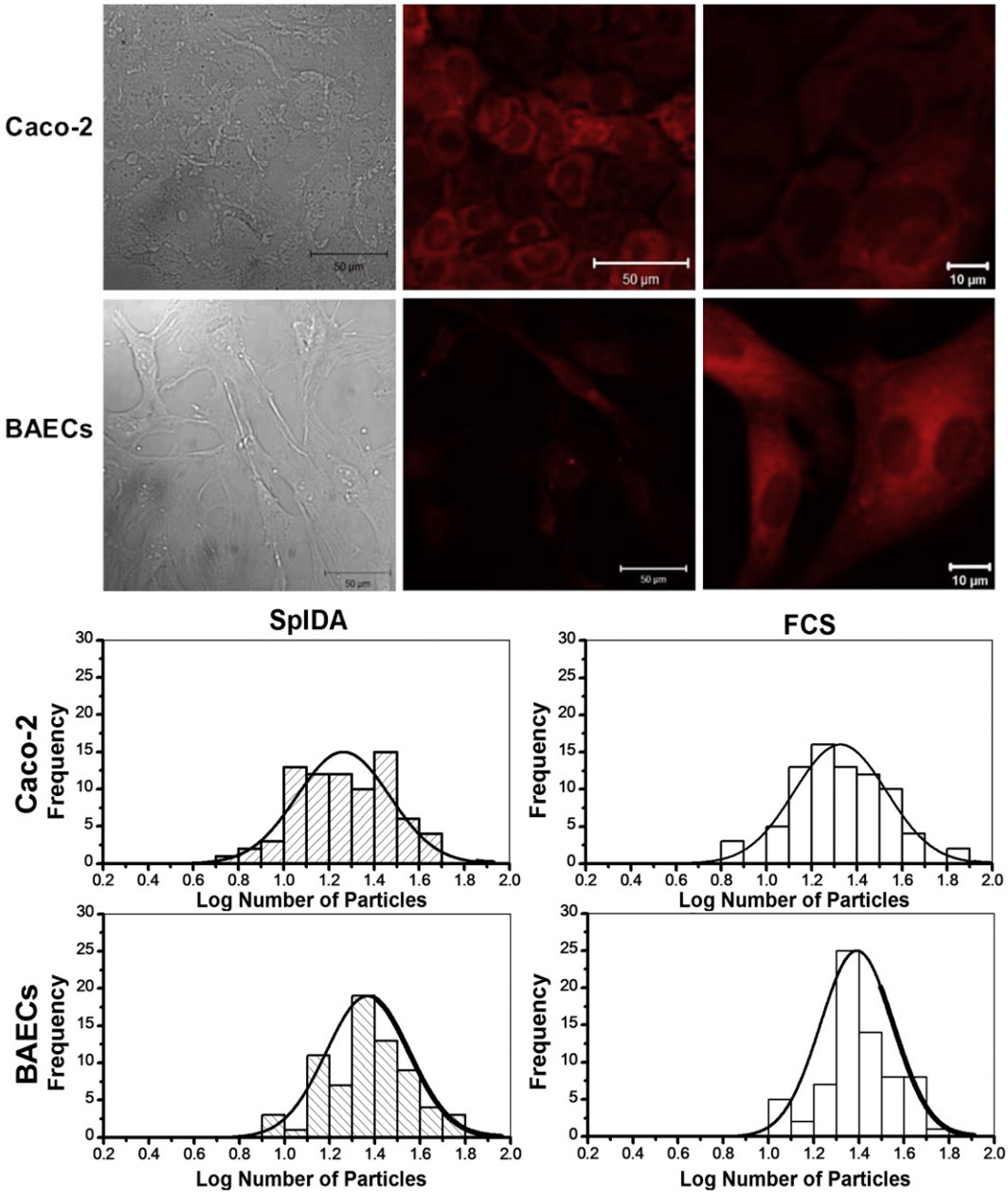


**Fig. 6.** Confocal images of Caco-2 cells (top) and BAECs (bottom) incubated with 50 nM CellTrace™ calcein red-orange AM for 60 min. Images of 0.44 (left and centre) and 0.07 μm (right) pixel size acquired from each cell line—all other imaging parameters were kept constant. Corresponding log number of CellTrace™ calcein red-orange (AM) particles in Caco-2 cells and BAECs incubated with 50 nM CellTrace™ calcein red-orange AM concentration for 60 min ($n = 70$) following SpIDA (left) and FCS (right) measurements. The data was binned in OriginPro (bin size 0.1), a histogram constructed and fitted to a normal distribution (represented by a solid line).

inter- and intracellular heterogeneity in the range of detected intracellular number of particles (Fig. 7).

Initial assessment of fluorescence intensities for both cell lines indicated concentration-dependent behaviour with a higher extent of retention in Caco-2 monolayers. The influence of fluorophore concentration on the intracellular number of particles detected demonstrated complementarity between SpIDA-acquired number of particles and FCS measurements (please note that data for 100 nM CellTrace™ calcein red-orange (AM) in BAECs could not be included due to saturation of the avalanche photodiode detector during FCS experiments). Performance of a single factor ANOVA test ($P < 0.05$) in all cases confirmed no statistically significant differences between the number of particles obtained from FCS measurements and SpIDA analysis of confocal images in each cell line.

## 4. Discussion

Assessment of ligand internalisation with bulk 'black-box' methods (e.g. fluorescence plate readers) applied to *in vitro* cell models provides a macroscopic evaluation of an 'apparently homogeneous ensemble' with limited information on intricate compartmentalised distributions in individual cells and within cell populations [22]. In order to provide a more in-depth understanding of cellular uptake, evaluation at a microscopic level could be more insightful in profiling the intracellular concentration of a compound, and sub- and inter-cellular distributions [8,23].

Therefore, the intention of this study was to microscopically probe the intracellular accumulation of a model fluorescent compound, CellTrace™ calcein red-orange (AM), in Caco-2 and BAEC cell monolayers

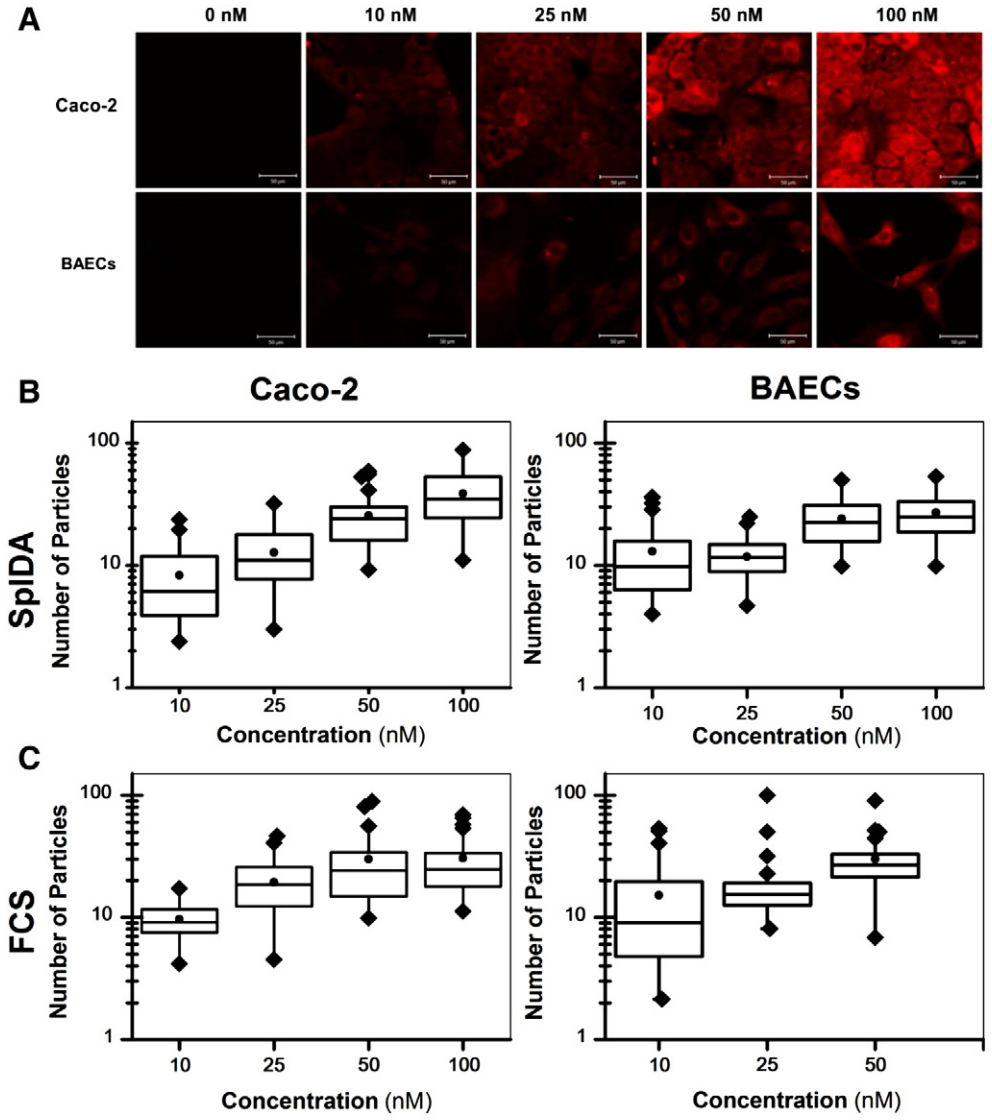


**Fig. 7.** Confocal images of CellTrace™ calcein red-orange (AM) in Caco-2 cells and BAECs (512 × 512 pixels and 0.44 μm pixel size) following incubation with various concentrations of CellTrace™ calcein red-orange AM for 60 min (A) number of particles determined using SpIDA (B) and FCS (C) (n = 25). The mean number of particles is represented by (●), outliers (◊), and the median, upper and lower quartiles are represented by horizontal lines.

using FCS in combination with live cell imaging, and image analysis tools to enable quantification of intracellular fluorophore uptake kinetics and profiling intracellular distributions.

Preliminary assessment of CellTrace™ calcein red-orange AM behaviour in solution using FCS revealed that this compound exhibited the appropriate fluorescence characteristics (e.g. triplet time, count rate and profile) for cellular FCS studies (see Fig. 3). Subsequently, FCS measurements, confocal imaging and SpIDA were applied to the determination of intracellular accumulation of CellTrace™ calcein red-orange (AM) as a function of concentration (see Fig. 7) and period of incubation in Caco-2 and BAEC cell monolayers (see Fig. 5).

Confocal images subjected to SpIDA were acquired under identical conditions (e.g. cell passage, incubation time and fluorophore concentration) to FCS experiments and resultant output data compared against that of FCS measurements.

The wealth of data that can be extracted from fluorescent confocal images of cellular uptake or biophysical studies often remain under-exploited. Here, the analysis of mean fluorescence intensities of fluorophore in cell populations, a routine tool for the bulk characterisation of fluorescent phenomena in black-box approaches, was compared to trends observed in the intracellular concentration of CellTrace™ calcein red-orange (AM) in both cell lines.

These plots confirmed time (see Fig. 5) and concentration-dependent (see Fig. 7) behaviour of CellTrace™ calcein red-orange (AM) uptake into both cell lines with an apparent higher extent of CellTrace™ calcein red-orange (AM) accumulation in Caco-2 compared to BAECs, while FCS and SpIDA measurements indicated otherwise. Fluorescence intensity is a product of number of particles and quantal brightness (of the fluorophore); hence, a higher quantal brightness of CellTrace™ calcein red-orange (AM) in the Caco-2 cell cytoplasm could potentially contribute to the observed higher fluorescence intensity and extent of accumulation in this cell line using this approach [24]. Furthermore, intracellular population distributions calculated using SpIDA and FCS measurements exhibited broad intra- and intercellular heterogeneity, an aspect that the current application of black box approaches is unable to address.

Following an extended period of incubation (i.e. 60 min) with CellTrace™ calcein red-orange AM (Fig. 6), a statistically significant

($P < 0.05$) difference was noted in the intracellular concentration ranges of CellTrace™ calcein red-orange (AM) for both cell lines. These observations may be attributed to differences in plasma membrane composition and the available surface area exposed to CellTrace™ calcein red-orange AM for uptake, or esterase activity levels based on the morphological and phenotypic differences between BAECs (endothelial) and Caco-2 (epithelial) cells.

Despite providing an accurate measure of concentration in an optimised setup, a common challenge encountered with FCS as a well-established biophysical tool in monitoring temporal intracellular concentration fluctuations, is the labour-intensive process of optimising intracellular positioning within single cells and performance of sufficient repeat measurements to ensure generation of a statistically representative sample set. Additionally, photobleaching and photo-damage may occur due to sustained exposure of the cell sample to static confocal volumes.

Over the recent decade, dynamic approaches exemplified SpIDA [8] and number and brightness analysis [25] have been developed that overcome some of these limitations, and through optimisation of scan speed and image acquisition parameters can accurately quantify parameters such as concentration, dynamics or the oligomerisation status of fluorophores in intracellular compartments.

An added advantage of SpIDA application as a spatial tool in profiling intracellular concentrations over methods that rely on temporal measurements (e.g. FCS) [7] is the minimisation of photobleaching effects, since single confocal images can be analysed and the rapid acquisition of data over multiple fields of view enables rapid profiling of cell populations (in contrast to laborious single cell measurements to generate statistically-relevant cell populations). In comparison to FCS, acquisition and analysis of confocal images with SpIDA do not require a specialist setup and can simply be performed with a commercial confocal microscope [8]. Furthermore, the scope exists to subject the same image set to several image analysis tools in order to extensively probe the inherent information contained within confocal images and analyse image sets acquired in three dimensions.

Data obtained from profiling the intracellular concentration of CellTrace™ calcein red-orange (AM) as a model compound in this study at '*proof of concept*' level highlights that image analysis tools can be utilised to generate meaningful parameters that can be insightful in the characterisation of intracellular distributions of fluorophores. Therefore, the scope exists to extend this work to the biophysical characterisation of ligand uptake and distribution, permitting concomitant qualitative assessment of cellular localisation and profiling distribution heterogeneities in more complex systems.

## 5. Conclusions

The internalisation and subsequent accumulation of CellTrace™ calcein red-orange (AM) following esterase cleavage were assessed utilising a combination of confocal image analysis and FCS measurements that exhibited complementarity across approaches used in a simple in vitro system at '*proof of concept*' level.

Data obtained from both FCS measurements and SpIDA of live cell images suggest concentration, time- and cell line-dependent intracellular accumulation of CellTrace™ calcein red-orange (AM) and enabled profiling of inter- and sub-cellular number of particle distributions within a population of cells. Analytical approaches (i.e. bulk black box methods) utilised in routine fluorescence-based trafficking studies profile transcellular transport at a macroscopic level providing little insight into compartmentalised events occurring at a microscopic level within the cell monolayer, and the biomolecular machinery recruited in intracellular trafficking.

With current image acquisition and analysis capabilities it is possible to non-invasively probe intracellular uptake and transport processes at a microscopic level. Rapid data acquisition from individual cells in the form of confocal images provides a platform for the concomitant assessment of sub-cellular and intercellular variability in both rate and extent of cellular trafficking. It is envisaged that with advances in image analysis algorithms and the development of novel image analysis tools in parallel with the increasing commercial availability of high content screening systems, ligand accumulation and multi-parametric assessment of kinetics and the extent of intracellular retention will become a reality in more complex transport models.

## Acknowlegement

The authors would like to thank the BBSRC and Manchester Alumni fund for supporting this project.

## Appendix A. Supplementary data

Supplementary data to this article can be found online at http://dx.doi.org/10.1016/j.bbagen.2014.05.014.

## References

[1] P. Artursson, J. Karlsson, Correlation between oral drug absorption in humans and apparent drug permeability coefficients in human intestinal epithelial (Caco-2) cells, Biochem. Biophys. Res. Commun. 175 (1991) 880–885.
[2] D. Magde, E. Elson, W.W. Webb, Thermodynamic fluctuations in a reacting system measurement by fluorescence correlation spectroscopy, Phys. Rev. Lett. 29 (1972) 705–708.
[3] P. Schwille, J. Korlach, W.W. Webb, Fluorescence correlation spectroscopy with single-molecule sensitivity on cell and model membranes, Cytometry 36 (1999) 176–182.
[4] Z. Földes-Papp, U. Demel, G.P. Tilz, Detection of single molecules: solution-phase single-molecule fluorescence correlation spectroscopy as an ultrasensitive, rapid and reliable system for immunological investigation, J. Immunol. Methods 260 (2002) 117–124.
[5] R. Ghosh, S. Sharma, K. Chattopadhyay, Effect of arginine on protein aggregation studied by fluorescence correlation spectroscopy and other biophysical methods, Biochemistry 48 (2009) 1135–1143.
[6] J. Ries, P. Schwille, Fluorescence correlation spectroscopy, BioEssays 34 (2012) 361–368.
[7] D. Kolin, P. Wiseman, Advances in image correlation spectroscopy: measuring number densities, aggregation states, and dynamics of fluorescently labeled macromolecules in cells, Cell Biochem. Biophys. 49 (2007) 141–164.
[8] A.G. Godin, S. Costantino, L.-E. Lorenzo, J.L. Swift, M. Sergeev, A. Ribeiro-da-Silva, Y. De Koninck, P.W. Wiseman, Revealing protein oligomerization and densities in situ using spatial intensity distribution analysis, Proc. Natl. Acad. Sci. 108 (2011) 7010–7015.
[9] C.A. Schneider, W.S. Rasband, K.W. Eliceiri, NIH Image to ImageJ: 25 years of image analysis, Nat. Methods 9 (2012) 671–675.
[10] F. de Chaumont, S. Dallongeville, N. Chenouard, N. Herve, S. Pop, T. Provoost, V. Meas-Yedid, P. Pankajakshan, T. Lecomte, Y. Le Montagner, T. Lagache, A. Dufour, J.-C. Olivo-Marin, Icy: an open bioimage informatics platform for extended reproducible research, Nat. Methods 9 (2012) 690–696.
[11] P. Furrer, R. Gurny, Recent advances in confocal microscopy for studying drug delivery to the eye: concepts and pharmaceutical applications, Eur. J. Pharm. Biopharm. 74 (2010) 33–40.
[12] Z. Xiaobo, S.T.C. Wong, High content cellular imaging for drug development, IEEE Signal Proc. Mag. 23 (2006) 170–174.
[13] P. Lang, K. Yeow, A. Nichols, A. Scheer, Cellular imaging in drug discovery, Nat. Rev. Drug Discov. 5 (2006) 343–356.
[14] M. Sergeev, Measurement of Oligomerization States of Membrane Proteins via Spatial Fluorescence Intensity Fluctuation Analysis, Department of Physics, McGill University, Montreal, 2010.
[15] J.L. Swift, A.G. Godin, K. Doré, L. Freland, N. Bouchard, C. Nimmo, M. Sergeev, Y. De Koninck, P.W. Wiseman, J.-M. Beaulieu, Quantification of receptor tyrosine kinase transactivation through direct dimerization and surface density measurements in single cells, Proc. Natl. Acad. Sci. 108 (2011) 7016–7021.
[16] K. Whitehead, N. Karr, S. Mitragotri, Safe and effective permeation enhancers for oral drug delivery, Pharm. Res. 25 (2008) 1782–1788.
[17] P. Artursson, C. Magnusson, Epithelial transport of drugs in cell culture II: effect of extracellular calcium concentration on the paracellular transport of drugs of different lipophilicities across monolayers of intestinal epithelial (Caco-2) cells, J. Pharm. Sci. 79 (1990) 595–600.
[18] P. Artursson, K. Palm, K. Luthman, Caco-2 monolayers in experimental and theoretical predictions of drug transport, Adv. Drug Deliv. Rev. 46 (2001) 27–43.
[19] Invitrogen, Acetoxymethyl (AM) and Acetate Esters, 2010.
[20] D.S. Banks, C. Fradin, Anomalous diffusion of proteins due to molecular crowding, Biophys. J. 89 (2005) 2960–2971.
[21] J. Widengren, U. Mets, R. Rigler, Fluorescence correlation spectroscopy of triplet states in solution: a theoretical and experimental study, J. Phys. Chem. 99 (1995) 13368–13379.

[22] S.A. Kim, P. Schwille, Intracellular applications of fluorescence correlation spectroscopy: prospects for neuroscience, Curr. Opin. Neurobiol. 13 (2003) 583–590.
[23] P. Schwille, U. Haupts, S. Maiti, W.W. Webb, Molecular dynamics in living cells observed by fluorescence correlation spectroscopy with one- and two-photon excitation, Biophys. J. 77 (1999) 2251–2265.
[24] M.A. Digman, R. Dalal, A.F. Horwitz, E. Gratton, Mapping the number of molecules and brightness in the laser scanning microscope, Biophys. J. 94 (2008) 2320–2332.
[25] R.B. Dalal, M.A. Digman, A.F. Horwitz, V. Vetri, E. Gratton, Determination of particle number and brightness using a laser scanning confocal microscope operating in the analog mode, Microsc. Res. Tech. 71 (2008) 69–81.